Journal of Polymers and the Environment (2020) 28:2669–2680
https://doi.org/10.1007/s10924-020-01806-8

ORIGINAL PAPER

All-Biomass Double Network Gel: Highly Efficient Removal of Pb^{2+} and Cd^{2+} in Wastewater and Utilization of Spent Adsorbents

Lan Wen[1,2] · Yuanmeng Zhang[1] · Chengbin Liu[1] · Yanhong Tang[3]

Published online: 27 June 2020

Abstract

Besides excellent adsorption performance of adsorbents, the disposal of spent adsorbents should be considered for environmental concern. In this study, a new all-biomass double network Jute/sodium alginate (Jute/SA) gel is prepared via the simple dripping technique. 80 wt% water of Jute/SA hydrogel endows the adsorbent with high permeability for heavy metal ions diffusion onto internal adsorption sites. The Jute/SA gel adsorbent can efficiently remove heavy metals from melting wastewater, especially Pb^{2+} and Cd^{2+}. The adsorbent shows high adsorption capacities of 291.3 mg g^{-1} for Pb^{2+} and 149.9 mg g^{-1} for Cd^{2+} at 298 K. The adsorption equilibrium reaches within 45 min for 45 mg L^{-1} Cd^{2+} and Pb^{2+} using 1 g L^{-1} adsorbent, showing 98% removal efficiency of Pb^{2+} and Cd^{2+}. Moreover, the removal efficiencies in 45 min reach up to 99.1% for Pb^{2+} (7.539 mg L^{-1}) and 89.9% for Cd^{2+} (4.743 mg L^{-1}) in actual melting effluent containing Zn (43.95 mg L^{-1}), Cu (16.50 mg L^{-1}), Mn (19.24 mg L^{-1}), Ni (4.90 mg L^{-1}) and Fe (33.75 mg L^{-1}) using 1 g L^{-1} adsorbent. The concentrations of Pb and Cd decrease below 0.001 mg L^{-1} using 4 g L^{-1} adsorbent. Furthermore, the adsorption efficiencies for Pb^{2+} and Cd^{2+} remain above 95% in the tenth cycle, and the desorption efficiency is up to 99%. In addition, the spent Jute/SA gel was a good organic fertilizer for plant growth. This work develops an efficient and eco-friendly biomass adsorbent for the removal of heavy metals in actual wastewater.

Keywords Biomass adsorbent · Heavy metals · Melting wastewater · Fertilizer

Introduction

Heavy metal contaminants in water and disposal of spent heavy metal adsorbents have been an environmental concern. The excessive discharge of wastewater containing lead (Pb^{2+}) and cadmium (Cd^{2+}) into aquatic environment may lead to a potential risk [1]. Adsorption technique is widely used to eliminate heavy metals in wastewater [2, 3]. Various adsorbent materials such as ion-exchange resins, carbon nanotubes and activated carbon have been extensively developed [4–6]. The adsorption process of heavy metal cations commonly involves boundary layer and intraparticle diffusion, as well as surface adsorption [7]. However, traditional compact granular adsorbents show a limited ion diffusion through pores. For example, the adsorption equilibrium time for activated carbon requires at least several hours [8]. In addition, the adsorption capacities of granular adsorbents are reluctantly discounted due to the pore blocking and burial of surface adsorption sites with the proceeding of adsorption [9]. Although nano-sized adsorbents show off faster adsorption, it is cumbersome for fine adsorbents to separate, leading to extra operation cost and potential threat to environment [10]. Low-cost and high-performance (high adsorption capacity, fast adsorption, and good recyclability) adsorbents are highly demanded for practical applications.

Polymer hydrogels with an interpenetrating network structure possess a high water permeability for ion diffusion

✉ Chengbin Liu
chem_cbliu@hnu.edu.cn

✉ Yanhong Tang
tangyh@hnu.edu.cn

1 Hunan Provincial Key Laboratory for Cost-Effective Utilization of Fossil Fuel Aimed at Reducing Carbon-dioxide Emissions, State Key Laboratory of Chemo/Biosensing and Chemometrics, Hunan University, Changsha 410082, People's Republic of China

2 Department of Agriculture and Medical Science, Hunan Radio and TV University, Changsha 410004, People's Republic of China

3 College of Materials Science and Engineering, Hunan University, Changsha 410082, People's Republic of China

into polymer frameworks. Some hydrogel adsorbents have been used to remove heavy metals in water. These polymer hydrogels were synthesized by polymerization of olefin monomers containing hydrophilic functional groups [11]. However, the disposal of spent adsorbents is an environmental concern due to the non-biodegradation of polyolefin polymers. In contrast, biodegradable biomass materials are attractive [12]. Conventional biomass hydrogels, however, are generally too weak and viscous to recycle. Some measures have to be taken to enhance the mechanical strength of biomass hydrogels, such as chemical crosslinking, synthetic polymer introduction and inorganic hybridization [13–16]. However, these modified bulk biomass-based adsorbents suffer reduced biodegradability, decreased adsorption capacity and increased use cost. The utilization of spent adsorbents is generally ignored. All-biomass adsorbents with both good adsorption performance and post-utilization are highly desired.

In this study, a new all-biomass double network jute/sodium alginate (Jute/SA) gel was prepared via the simple dripping technique. Both jute and sodium alginate are readily available biomass materials. The chains of Jute and SA were cross-linked together into a stable bead structure through the electrostatic interaction and hydrogen bonds. The high water permeability (80 wt%) endowed Jute/SA hydrogel with accessible channels for heavy metal ions diffusion into the adsorbent, which would ensure the utilization of adsorption sites as much as possible. Thus, the Jute/SA gel adsorbent showed a highly efficient removal of heavy metals in wastewater with an excellent recyclability. Furthermore, the spent Jute/SA hydrogel adsorbent was a good organic fertilizer for plant growth.

Materials and Methods

Chemicals

Jute leaf powder (100 mesh) was provided by Institute of Bast Fiber Crops, Chinese Academy of Agricultural Sciences. Sodium alginate (SA) was purchased from Shanghai Aladdin Bio-Chem Technology Co., Ltd. Other chemicals were purchased from Sinopharm Chemical Reagent Co., Ltd. and used as received. The industrial melting effluent was taken from Hengyang Shuikoushan smelting plant. All aqueous solutions were prepared with deionized water unless otherwise stated.

Preparation of Jute/SA Hydrogel

The specific preparation process of Jute/SA gel is as follows: 1.0 g of jute powder was dissolved in 50 mL of 0.5 mol L^{-1} NaOH aqueous solution to get a ropy solution. 2.0 g of SA was dissolved in 100 mL deionized water to form a viscous solution. The two as-prepared solutions were mixed well under magnetic stirring. The mixed solution was dropped into a 200 mL of 6.0 wt% $Ca(NO_3)_2$ solution using a syringe (10 mL) to obtain spherical particles. The formed particles were further stabilized through domestication in the solution for 15 min. The collected particles were washed with deionized water several times to neutral to get Jute/SA hydrogel adsorbent. In addition, dried Jute/SA gel could be obtained through the freeze drying of Jute/SA hydrogel. The schematic diagram of Jute/SA hydrogel synthesis and network structure is shown in Scheme 1.

Characterization and Analysis Methods

The surface morphology and network structure of Jute/SA gel was observed using a scanning electron microscope (SEM, S-4800). Fourier transform infrared spectra (FTIR, Nicolet 5700) was used to determine the functional groups of Jute, SA and Jute/SA gel. The surface chemistry of Jute/SA gel before and after adsorbing heavy metals was determined by X-ray photoelectron spectroscope (XPS, K-Alpha 1063). The thermal stability of the Jute/SA gel was analyzed by thermogravimetric analysis (TGA, TG/DTA7300) under nitrogen atmosphere. The zero-charge point (pH_{PZC}) determination of Jute/SA gel was measured by ΔpH drift method in 0.01 mol L^{-1} NaCl solution [17].

Batch Adsorption Experiments

The Pb^{2+} and Cd^{2+} solutions with preselected concentrations were prepared by dissolving lead nitrate and cadmium nitrate in deionized water. The pH of the solutions was adjusted using a 0.1 mol L^{-1} HCl or NaOH aqueous solution, where the pH valves of Pb^{2+} and Cd^{2+} solutions were adjusted to 5.0 and 6.0 for adsorption experiments, respectively. Nitrates (K^+, Na^+, Mg^{2+}, Ca^{2+}, Zn^{2+}, Ni^{2+}, Cu^{2+} or Mn^{2+}) or humic acid (HA) was separately added as background substances with a preset concentration. Jute/SA aerogel (1.0 g L^{-1}) was added to the heavy metal solution at predetermined concentration, and the reaction was carried out at room temperature (ca. 25 °C) with shaking at 160 r min^{-1} until adsorption equilibrium, and then the supernatant was collected. The concentration of heavy metal ions in the initial solution and the solution after the reaction was measured by atomic absorption spectrometer (AAS, Hitachi Z-2000). For the regeneration study, the metal-adsorbed hydrogel was eluted with 0.1 mol L^{-1} HCl solution, and then regenerated with 0.1 mol L^{-1} NaOH solution (pH 13) followed by washing with deionized water to neutral.

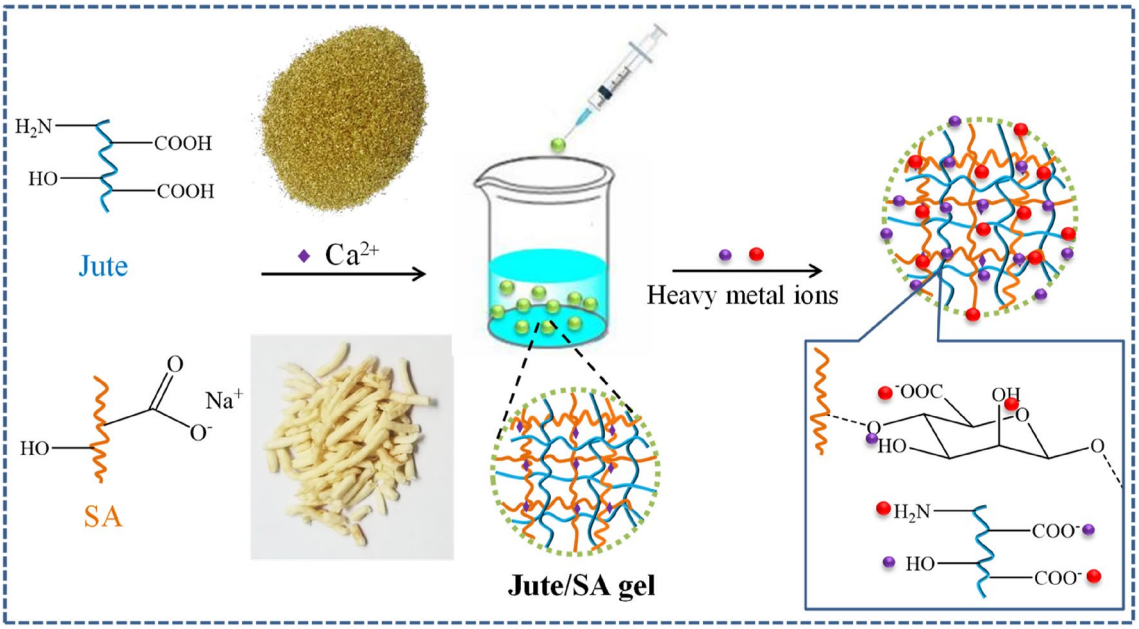

Scheme 1 Schematic diagram of Jute/SA hydrogel synthesis and network structure

Data Analysis

The adsorption data were fitted by two kinetic models (pseudo-first-order and pseudo-second-order equations) and three types of isotherms (Langmuir, Freundlich and Dubinin–Radushkevich (D–R) models). The adsorption percentage (sorption $\% = (C_0 - C_e)/C_0 \times 100$) and partition coefficient ($K_d = (C_0 - C_e)/C_e \times V/m$) were calculated by dividing the initial concentration (C_0) and the equilibrium concentration (C_e), where V represents the volume of the heavy metal solution and m represents the mass of Jute/SA. All experimental data are the average value after repeated measurement at least three times, and the relative errors were less than 5%.

Plant Cultivation Experiments

The seed of *Solanum nigrum* L. was purchased from Hebei Qingfeng Seed Industry, China. The spent Jute/SA hydrogel was washed to remove heavy metal ions for use as fertilizer. Roseite and spent Jute/SA hydrogel (wt% ratio of 60/40, total mass of 800 g for one basin) were mixed well and used as the cultivation medium. Five seeds were sowed into the medium in one cultivation basin. The temperature was ca. 28 °C for daytime and ca. 25 °C for night in a training room. Three 300 W Xe lamps were used as simulated sunlight. The focused intensity on the plant was 120 mW cm^{-2}. They were watered using tap water every two days. After 2 weeks, only one yang tree in one basin was retained and others were removed. As a control, the growth of *Solanum nigrum* L. was only in roseite cultivation medium but watered using Hoagland's nutrient solution (Hoagland's nutrient solution: $Ca(NO_3)_2{\cdot}4H_2O$ (0.005 mol L^{-1}), KNO_3 (0.005 mol L^{-1}), $MgSO_4{\cdot}7H_2O$ (0.002 mol L^{-1}), KH_2PO_4 (0.001 mol L^{-1}) and H_2O).

Results and Discussion

Characterizations

The Jute/SA hydrogel was prepared as shown in Scheme 1. The chains of Jute and SA were cross-linked into a stable bead structure through the electrostatic interaction (between Ca^{2+} cations and oxygen-containing anionic groups) and hydrogen bonds (–O–H···O(N)). During the swelling process in water, the gel reached a swelling equilibrium within about 8.0 h and the swelling ratio was about 3.1 (from about 1 mm for freeze-dried gel to approximately 3 mm for hydrogel) (Fig. 1a), which contained about 80 wt% water in hydrogel and kept a stable bead structure due to the cross-linking of the chains by electrostatic interaction and hydrogen bonds. Moreover, the freeze-dried Jute/SA gel was a porous aerogel (top left, Fig. 1a). The porous structure and high water permeability endowed Jute/SA hydrogel with accessible channels for heavy metal ions diffusion into the adsorbent, which would ensure the utilization of adsorption sites as much as possible. The FTIR spectra of the samples are shown in Fig. 1b. SA exhibited characteristic absorption peaks at around 1628 cm^{-1} and 1423 cm^{-1} ascribed to symmetric stretching vibration and

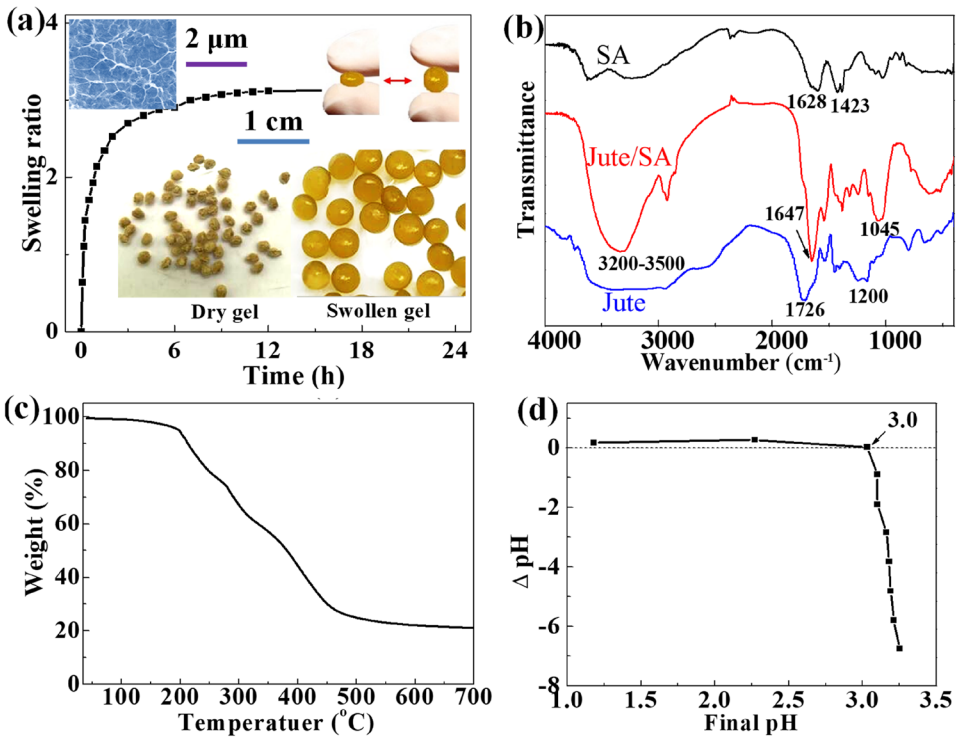

Fig. 1 Swelling equilibrium of Jute/SA gel (**a**) (top left is the SEM image of freeze-dried Jute/SA), FT-IR spectra of SA, Jute and Jute/SA (**b**), TGA curve of Jute/SA aerogel (**c**), and pH_{pzc} of Jute/SA gel (**d**)

antisymmetric stretching vibration for $–COO^-$ in SA, respectively [18]. After gelation of Jute and SA in the presence of Ca^{2+} cations, the absorption peaks of $–COO^-$ in Jute/SA gel became stronger and shift slightly compared to those in SA, possibly due to the introduction of more $–COO^-$ from Jute and the electrostatic interaction. In contrast, the absorption peak (1647 cm^{-1}) of C=O in Jute/SA occurred blue shit compared with that (1726 cm^{-1}) in Jute, which was due to the decrease in electron cloud density of C=O after the introduction of Ca^{2+} cations. Moreover, there was a broad absorption band in the range of 3200–3500 cm^{-1} in Jute and Jute/SA, due to the stretching vibration of –OH and $–NH_2$ functional groups [19]. In addition, the strong absorption peak at around 1045 cm^{-1} for C–O stretching vibration in Jute/SA should be due to the formation of more hydrogen bonds of –O–H···O(N) after crosslinking [20]. The TGA result indicated that Jute/SA gel was highly stable below 150 °C (Fig. 1c), meeting the need of actual application. The zero-charge point (pH_{PZC}) of Jute/SA was about 3.0 (Fig. 1d). The pH_{PZC} plays an important role in determining the surface charge and adsorption capacity of adsorbents. The presence of H^+ or OH^- ions in the solution may alter the potential surface charge of the adsorbent. When changing the pH, there will appear ΔpH drift. If the pH of the solution is below its pH_{PZC}, the negative charges (OH^-) will deviate from the surface of adsorbent. Conversely, if the pH is above its pH_{PZC}, the positive charges (H^+) will deviate from the surface of adsorbent companying the adsorption of cations from electrolytes. Thus, when the pH value of the solution is above 3.0, the surface of Jute/SA will be available for the adsorption of heavy metal cations by electrostatic interactions.

Adsorption Selectivity of Jute/SA Gel

The adsorption selectivity is important to evaluate the adsorption capacity for targeted heavy metals. The adsorption experiment was conducted in a solution containing one kind of interfering metal ion (Pb^{2+}, Cd^{2+}, Zn^{2+}, Mn^{2+}, Ni^{2+} or Cu^{2+}) which commonly exist in practical melting effluent. The initial concentration of each metal ion was 0.25 mmol L^{-1} (52, 28, 16.5, 14, 14.5, and 16 mg L^{-1} for Pb^{2+}, Cd^{2+}, Zn^{2+}, Mn^{2+}, Ni^{2+} and Cu^{2+}, respectively). The initial pH of the solution was 5.0. As shown in Fig. 2, the removal efficiency of Pb^{2+} and Cd^{2+} reached 97.7% and 89.6% in 45 min, respectively, which was much higher than that for other interfering metal ions.

The adsorption selectivity can be expressed by selectivity coefficient ($\beta Pb^{2+}/M^{2+}$) (Eq. 1):

$$\beta Pb^{2+}/M^{2+} = D_{Pb^{2+}}/D_{M^{2+}} \quad (1)$$

where, D is the distribution coefficient which can be calculated by Eq. 2:

$$D = (C_0 - C_e) \cdot V/(C_0 \cdot m) \quad (2)$$

where, C_0 and C_e are the concentrations of metal ions before and after adsorption (mol L^{-1}), V is solution volume (L), and m is adsorbent mass (g).

Table 1 Selective parameters of Jute/SA gel for heavy metals

Metal ion	Distribution coefficient (D) ($L\ g^{-1}$)	Selectivity coefficient ($\beta Pb^{2+}/M^{2+}$) ($\beta_{Pb^{2+}/M^{2+}}$)
Pb^{2+}	42.5	1
Cd^{2+}	8.6	0.2
Cu^{2+}	3.8	0.1
Zn^{2+}	0.8	0.02
Mn^{2+}	0.3	0.007
Ni^{2+}	0.03	0.0007

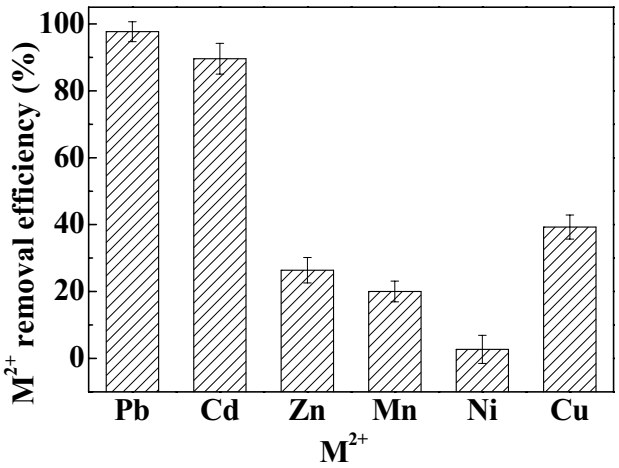

Fig. 2 Selective adsorption of Jute/SA gel. Conditions: C_0 = 0.25 mmol L^{-1} for each metal ion, pH 5.0, t = 45 min, T = 298 K, m/V = 1.0 g L^{-1}

The calculated results are listed in Table 1. The selectivity coefficients of the Jute/SA gel for Pb^{2+} and Cd^{2+} were 1 and 0.2, respectively, much higher than those for other ions. The removal efficiency priority was $Pb^{2+} > Cd^{2+} > Cu^{2+} > Zn^{2+} > Mn^{2+} > Ni^{2+}$. The selectivity is related to ion valence, stability constants, hydration radii, mass-to-charge ratio, and coordination capacity [21]. Thereby, the adsorption of Pb^{2+} and Cd^{2+} on Jute/SA gel was further investigated.

Effect of Environmental Conditions

The factors of pH value, background ions and HA in solution usually affect the surface chemistry (surface charge and ion states) of adsorbents. In order to investigate the effect of pH value on the adsorption of Pb^{2+} and Cd^{2+} by Jute/SA gel, a series of pH values were selected to carry out adsorption experiments (Fig. 3a, b). Under strong acidic conditions, high-concentration H^+ could compete with heavy metal ions for adsorption sites. Even so, the adsorption efficiency of Pb^{2+} and Cd^{2+} should be boasted in a pH range of 2–3 (pH_{PZC} of 3.0). The results indicate that chemosorption dominantly contributed to the adsorption behavior. With the increase of pH above 3.0, the electrostatic adsorption force became stronger, resulting in higher adsorption efficiencies of Pb^{2+} and Cd^{2+}. At pH 5.0 and 6.0, the adsorption efficiencies for Pb^{2+} and Cd^{2+} reached a maximum of 99.1% and 98.8%, respectively. When further increasing the pH to 6.2 for Pb^{2+} or 8.6 for Cd^{2+}, precipitation would occur at the pH of bulk solution precipitation (pH_{BSP} for 50 mg L^{-1}). Therefore, the adsorption on Jute/SA could be well conducted in

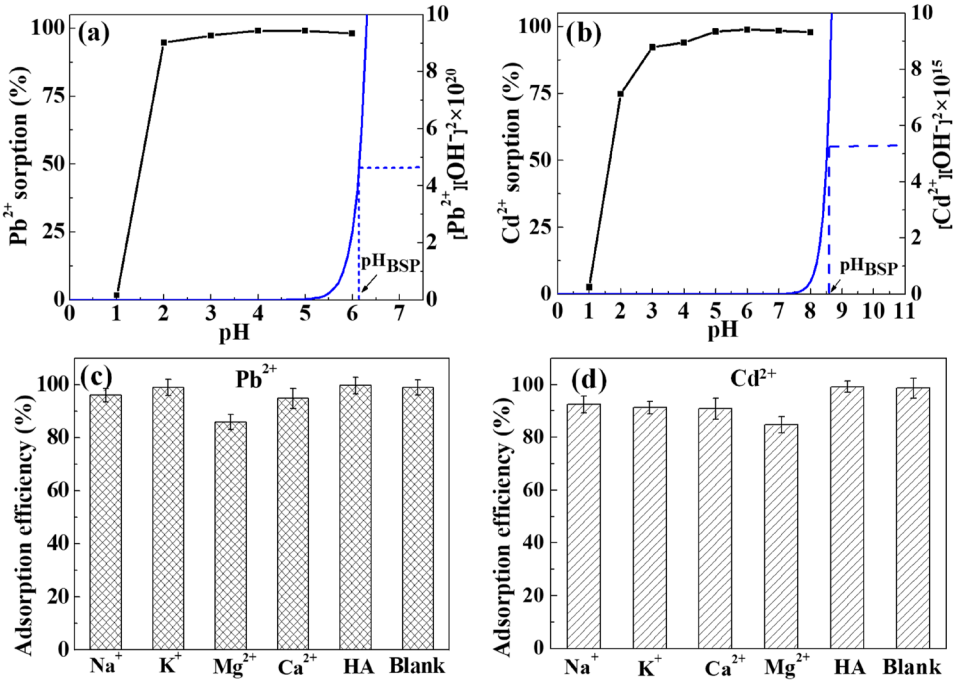

Fig. 3 Effect of environmental conditions on Pb^{2+} (**a**, **c**) and Cd^{2+} (**b**, **d**) adsorption by Jute/SA gel. Conditions: C_0 = 50 mg L^{-1}, t = 45 min, T = 298 K, m/V = 1.0 g L^{-1}, pH 5.0 for **c** and 6.0 for **d**

a wide pH range of 3–6 for Pb^{2+} or 3–8 for Cd^{2+} at a high concentration level of 50 mg L^{-1}.

The common cations (K^+, Na^+, Ca^{2+}, and Mg^{2+}) and humic acid (HA, $C_9H_9NO_6$) in aquatic system may compete with heavy metal ions at the adsorption sites of the adsorbents. The concentration of interfering substances was set at 0.01 mol L^{-1} (230, 391, 243, 400, and 2271 mg L^{-1} for Na^+, K^+, Mg^{2+}, Ca^{2+}, and HA, respectively) much higher the initial concentration of Pb^{2+} and Cd^{2+} (50 mg L^{-1}). As shown in Fig. 3c, d, HA had a negligible effect on the adsorption of Pb^{2+} and Cd^{2+}. K^+, Na^+ and Ca^{2+} had little effect on Pb^{2+} adsorption and a little effect on Cd^{2+} adsorption. In contrast, Mg^{2+} had an obvious effect on adsorption of both Pb^{2+} and Cd^{2+}. The influence of ionic species followed the sequence: $Mg^{2+} > Ca^{2+} > K^+ \approx Na^+$, probably due to the difference in electronegativity (0.82 for K^+, 0.93 for Na^+, 1.00 for Ca^{2+}, 1.31 for Mg^{2+}) and Hard Soft Acid Theory [22]. The declined adsorption efficiency could be due to the competition and electrostatic repulsion among metal ions as well as the lowered activity coefficient of Cd^{2+} and Pb^{2+} at a high ionic strength [23].

Adsorption Kinetics

Only 45 min was required to reach adsorption equilibrium with 98% removal efficiencies of Pb^{2+} and Cd^{2+} ($C_0 = 45$ mg L^{-1}, $m/V = 1$ g L^{-1}) (Fig. 4). The fast adsorption should be attributed to plenty of adsorption sites and high permeability of Jute/SA gel, which accelerated the diffusion of heavy metal ions.

The pseudo-first-order (Eq. 3) and pseudo-second-order (Eq. 4) models were used to describe the adsorption of Pb^{2+} and Cd^{2+} on Jute/SA gel.

$$Q_t = Q_e \cdot (1 - \exp(-k_1 t) \tag{3}$$

$$Q_t = Q_e \cdot \left(1 - 1/\left(1 + Q_e k_2 t\right)\right) \tag{4}$$

where, Q_t (mg g^{-1}) and Q_e are the adsorption capacity at time t and equilibrium, respectively; k_1 (L min^{-1}) and k_2 (g mg^{-1} min^{-1}) are the adsorption rate constants of pseudo-first-order and pseudo-second-order kinetic model, respectively. The correlation coefficients (R^2) of the pseudo-second-order kinetic model were a little larger than those of pseudo-first-order kinetic model (Table 2), indicating that both physical electrostatic adsorption and chemosorption was involved.

Adsorption Thermodynamics

In order to study the adsorption mechanism of Pb^{2+} and Cd^{2+} on Jute/SA gel, Langmuir and Freundlich isotherms were used to fit the adsorption data of Pb^{2+} and Cd^{2+} at 288, 298 or 308 K (Fig. 5).

Langmuir isotherms can describe a mono-layer adsorption behavior (Eq. 5).

$$Q_e = \frac{Q_m \cdot K_L \cdot C_e}{1 + K_L \cdot C_e} \tag{5}$$

Table 2 Adsorption kinetics parameters of Pb^{2+} and Cd^{2+} by Jute/SA gel

Metal ions	Pseudo-first-order model			Pseudo second-order model		
	k_1 (L min^{-1})	Q_e (mg g^{-1})	R^2	k_2 (g mg^{-1} min^{-1})	Q_e (mg g^{-1})	R^2
Pb^{2+}	0.13	43.83	0.9822	0.0043	44.40	0.9941
Cd^{2+}	0.15	44.39	0.9951	0.0048	44.81	0.9962

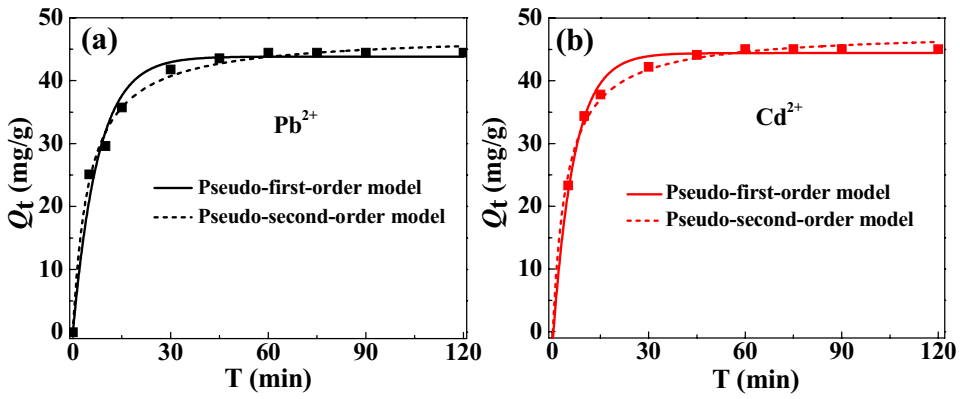

Fig. 4 Adsorption kinetics of Pb^{2+} and Cd^{2+} by Jute/SA gel. Conditions: $C_0 = 45$ mg L^{-1}, pH_{Pb} 5.0, pH_{Cd} 6.0, $T = 298$ K, $m/V = 1.0$ g L^{-1}

where, Q_e and C_e are the equilibrium adsorption capacity (mg g^{-1}) and equilibrium concentration (mg L^{-1}), respectively; Q_m is the maximum adsorption capacity (mg g^{-1}); K_L is adsorption constant (L mg^{-1}).

Freundlich isotherms can describe a heterogeneous adsorption process (Eq. 6).

$$Q_e = K_F \cdot C_e^{1/n_F} \quad (6)$$

where, K_F is adsorption constant ($mg^{1-n} L^{n/g}$) and n_F is Freundlich index.

The adsorption isotherms parameters are listed in Table 3. The correlation coefficient of Langmuir isotherm model was higher than that of Freundlich isotherm model, indicating that monolayered heavy metal ions were uniformly adsorbed onto the active sites. The adsorption capacity increased with increasing temperature, indicative of an endothermic reaction process. The Langmuir model predicted that the maximum theoretical adsorption capacities (Q_m) for Pb^{2+} and Cd^{2+} by Jute/SA gel at 298 K were 291.3 mg g^{-1} and 149.9 mg g^{-1}, respectively. For a bulk full-biomass adsorbent, it shows a comparable adsorption capacities for Pb^{2+} and Cd^{2+} with adsorbents reported (Table 4).

The thermodynamic parameters, Gibbs free energy difference (ΔG), enthalpy change (ΔH) and entropy change (ΔS) were calculated according to the van't Hoff equation. The thermodynamic parameters are listed in Table 5. The average free energy (E) was calculated by the Dubinin–Redushckevich (D–R) isotherm analysis (Fig. 5c, d). The E values for Pb^{2+} and Cd^{2+} adsorption were 13.4 and 12.7 kJ mol^{-1}, respectively, indicating that the adsorption involved a chemical reaction (E value between 8 and 16 kJ mol^{-1}) [24]. In addition, $\Delta G < 0$ and $\Delta H > 0$ indicated a spontaneous and endothermic adsorption process.

As a control, Langmuir and Freundlich isotherms were used to fit the adsorption data of Pb^{2+} by Jute and SA at 288, 298 or 308 K (Fig. 6). The Langmuir model predicted that the maximum theoretical adsorption capacities (Q_m) for Pb^{2+} by Jute and SA at 298 K were 224.6 mg g^{-1} and 177.0 mg g^{-1}, respectively, which were lower than that by Jute/SA gel. The possible reason may be ascribed to more available adsorption sites of porous double-network Jute/SA.

Table 3 Adsorption isotherms parameters of Pb^{2+} and Cd^{2+} on Jute/SA gel

Isothermal models	T (Pb^{2+}, pH 5.0)			T (Cd^{2+}, pH 6.0)		
	288 K	298 K	308 K	288 K	298 K	308 K
Langmuir model						
Q_m (mg g^{-1})	283.4	291.3	305.1	145.6	149.9	155.2
K_L (L mg^{-1})	0.300	0.261	0.300	0.714	0.822	1.095
R^2	0.9754	0.9802	0.9717	0.9663	0.9660	0.9670
Freundlich model						
K_F ($mg^{1-n} L^{n/g}$)	70.35	95.40	132.25	61.89	65.84	74.17
n_F	3.267	4.122	5.735	3.426	3.283	3.202
R^2	0.9459	0.9176	0.8665	0.9315	0.9385	0.9409

Table 4 Comparison of Q_m of adsorbents for Pb^{2+} and Cd^{2+}

Adsorbents	Experimental conditions	Q_m (mg g^{-1})		Ref.
		Pb^{2+}	Cd^{2+}	
Polyampholyte	pH_{Pb} 6.0, pH_{Cd} 7.0, T = 298 K	202.0	182.0	[15]
Amino functionalized starch	pH_{Pb} 5.0, pH_{Cd} 6.0, T = 313 K	256.4	180.0	[19]
Sodium polyacrylate/GO gel	pH 5.0, T = 303 K	238.3	–	[25]
Xanthate/magnetic chitosan	pH 5.0, T = 298 K	76.9	34.5	[26]
GAC/sodium titanate	pH 4.0, T = 298 K	250.0	149.0	[27]
Amino functionalized silica	pH 6.0, T = 298 K	194.4	190.5	[28]
Thiosemicarbazide/enonitrile	pH 6.4, T = 298 K	209.8	165.2	[29]
Mercapto-sepiolite	T = 298 K	116.3	34.8	[30]
Chitosan nanofiber	pH 5.0, T = 293 K	118.0	60.9	[31]
Activated carbon	pH 5.0, T = 303 K	123.4	70.8	[32]
Alginate gel pellet	T = 298 K	115.9	34.8	[33]
Ca^{2+}imprinted chitosan	pH 5.0, T = 298 K	47.1	49.9	[34]
Eucalyptus leaves	pH 5.0, T = 298 K	76.9	34.5	[35]
Jute/SA gel	pH_{Pb} 5.0, pH_{Cd} 6.0, T = 298 K	291.3	149.9	This work

Table 5 Adsorption thermodynamic parameters of Pb^{2+} and Cd^{2+} by Jute/SA gel

Metal ions	T (K)	ln(K^0)	ΔG^0 (kJ mol^{-1})	ΔS^0 (J mol^{-1} K^{-1})	ΔH^0 (kJ mol^{-1})
Pb^{2+} (pH 5.0)	288	2.85	− 6.69	173.9	43.62
	298	3.38	− 8.38		
	308	4.03	− 10.64		
Cd^{2+} (pH 6.0)	288	3.94	− 9.43	103.9	20.55
	298	4.14	− 10.25		
	308	4.49	− 11.51		

Adsorption Mechanism

According to Hard Soft Acid Base Theory, the acidity of Cd^{2+} is weaker than that of Pb^{2+} (acidity: K^+, Na^+ > Pb^{2+}, Cu^{2+} > Cd^{2+}, Cu^+). However, Jute/SA showed lower adsorption capacity for Cd^{2+} than Pb^{2+}. So the study on adsorption mechanism of Cd^{2+} on Jute/SA is important to design high-performance adsorbents for Cd^{2+} adsorption. The chemical groups and chemical environments of Jute/SA gel before and after the adsorption for Cd^{2+} were characterized by FTIR and XPS spectra. As shown in the FTIR spectra (Fig. 7a), after the adsorption for Cd^{2+} the absorption band in the range of 3200–3500 cm^{-1} for the stretching vibration of –OH/NH_2 functional groups was red-shifted. This change

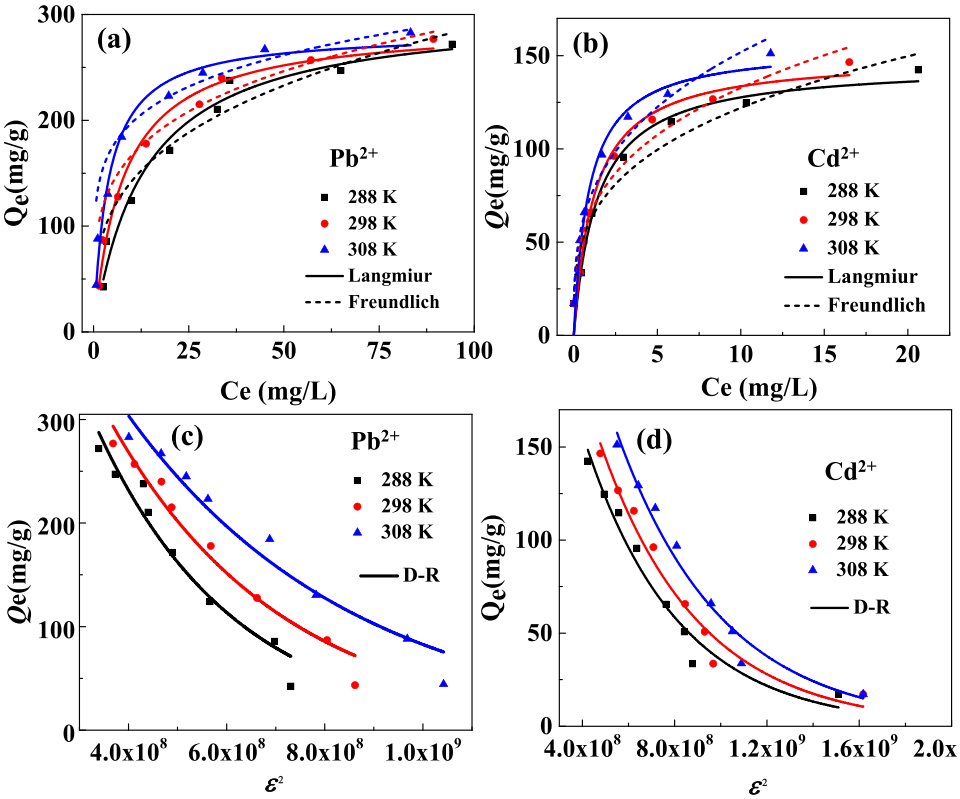

Fig. 5 Adsorption isotherms of adsorption for Pb^{2+} (**a**, **c**) and Cd^{2+} (**b**, **d**) by Jute/SA gel at different temperatures. Conditions: pH_{Pb} 5.0, pH_{Cd} 6.0, t = 45 min, m/V = 1.0 g L^{-1}

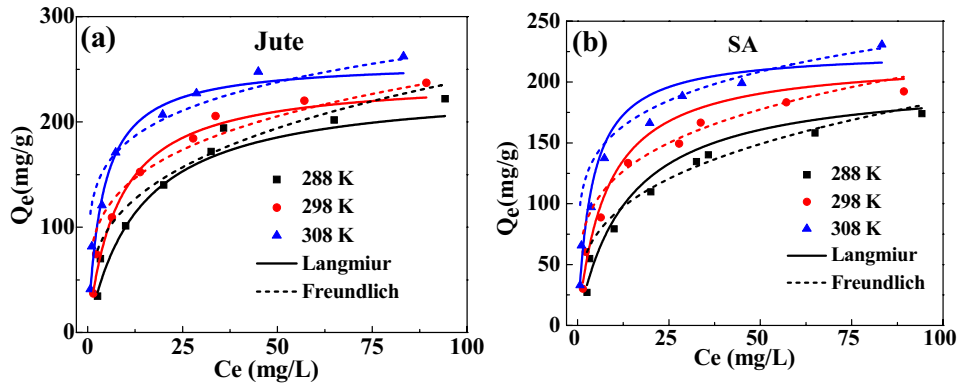

Fig. 6 Adsorption isotherms of adsorption for Pb^{2+} by Jute (**a**) and SA (**b**) at different temperatures. Conditions: pH 5.0, t = 45 min, m/V = 1.0 g L^{-1}

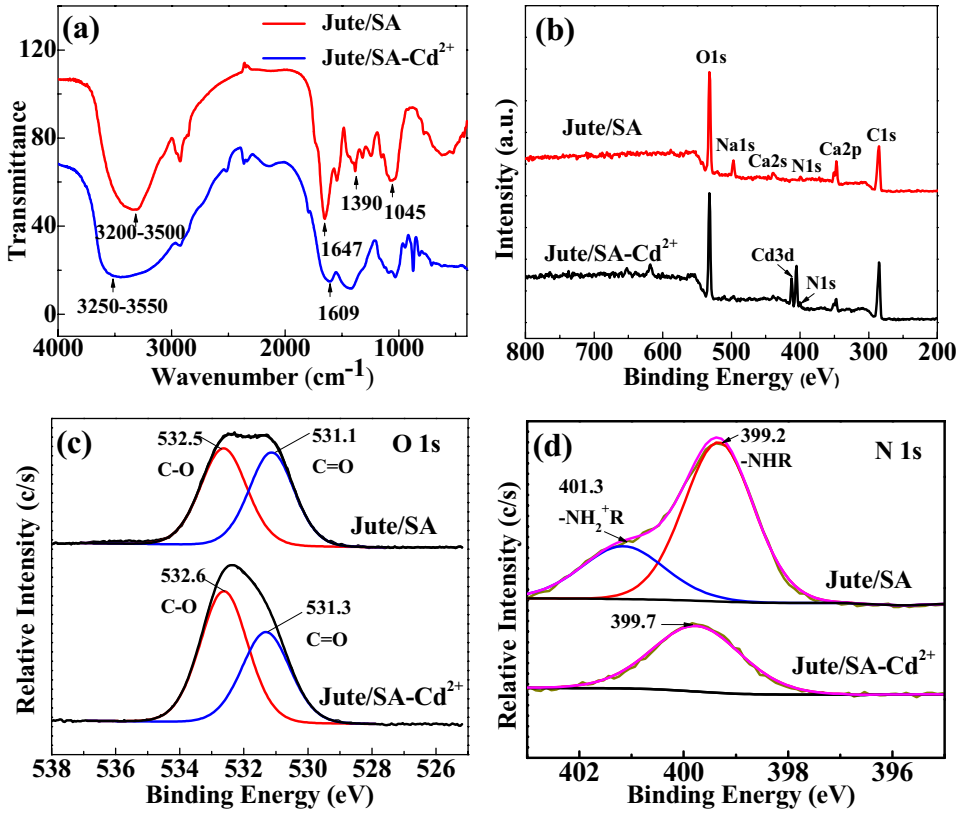

Fig. 7 FTIR (**a**), total XPS (**b**), O 1s HRXPS (**c**) and N 1s HRXPS (**d**) spectra of Jute/SA gel before and after adsorption of Cd^{2+}

may be caused by the coordination of Cd^{2+} with lone pair electrons of –OH/NH_2, resulting in reduced electron cloud density around these functional groups. In addition, the –COOH absorption peak at 1647 cm^{-1} shift to 1609 cm^{-1}, due to the ion exchange between H^+ and Cd^{2+}. Thereby, the main adsorption sites for Cd^{2+} were the carboxyl, hydroxyl and amino groups on Jute/SA gel. The XPS analysis of Jute/SA gel before and after adsorption of Cd^{2+} was further performed. After adsorption of Cd^{2+}, two peaks of Cd $3d_{5/2}$ (405.0 eV) and Cd $3d_{3/2}$ (411.0 eV) were clearly observed (Fig. 7b) [36]. The high resolution XPS (HRXPS) spectra of O 1s were analyzed (Fig. 7c). The adsorption of Cd^{2+} resulted in an increased binding energy of O in both C=O and C–O, due to the reduction of electron cloud density on O. Because of the coordination of Cd^{2+} with lone pair electrons of O atoms, the polarization of C=O and C–O bonds was strengthened, resulting in higher binding energy of C atoms adjacent to O atoms [37]. In addition, there appeared a new peak of N 1s at 399.7 eV after adsorbing Cd^{2+} (Fig. 7d), meaning a coordination of Cd^{2+} with N atoms. Moreover, the XPS peaks of Na^+ and Ca^{2+} became poor or disappeared. It is well known that (according to Hard Soft Acid Theory) heavy metal ions will be better complexed by carboxylic group than Na^+ or K^+. Therefore, the adsorption of heavy metal ions on Jute/SA gel was through the coordination between Cd^{2+} ions and –OH/NH_2 as well as the ion exchange between Cd^{2+} ions and other cations (H^+, Na^+ as well as Ca^{2+}). Taking into account the results of thermodynamics and pH effect together, chemosorption dominantly contributed to the adsorption behavior of Cd^{2+}. Strong electron-donating ability of functional groups in adsorbents is desired for capturing Cd^{2+}-like soft acid heavy metal ions.

Reusability of Jute/SA Gel and Utilization of Spent Adsorbent

Adsorbent reusability is critical to practical applications. The adsorption for Pb^{2+} and Cd^{2+} by Jute/SA gel was highly sensitive in the pH range from 1 to 3 (Fig. 3a, b). At low pH, Pb^{2+} and Cd^{2+} could be easily desorbed due to strong protonation and competitive effect with H^+. The metal ion-adsorbing Jute/SA gel was eluted with 0.1 mol L^{-1} HCl solution (pH 1) and regenerated with 0.1 mol L^{-1} NaOH solution (pH 13) followed by washing with deionized water to neutral (Fig. 8). The adsorption efficiencies for Pb^{2+} and Cd^{2+} were 99.1% and 98.8% in the first cycle and remained 96.1% and 95.3% in the tenth cycle, respectively. The desorption efficiency was higher than 99% in each cycle. Moreover, after 10 recycling processes, Jute/SA gel remained porous network structure (Fig. 9a) and exhibited good mechanical properties reflected in typical consecutive loading-unloading curves with gradually increased strain (Fig. 9b). These results indicated that the Jute/SA gel adsorbent had a good reusability.

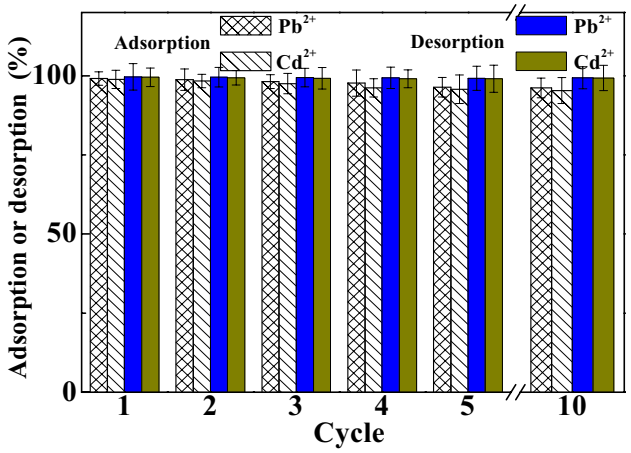

Fig. 8 Recycling of Jute/SA gel. Conditions: C_0 = 50 mg L^{-1}, pH_{Pb} 5.0, pH_{Cd} 6.0, t = 45 min, m/V = 1.0 g L^{-1}

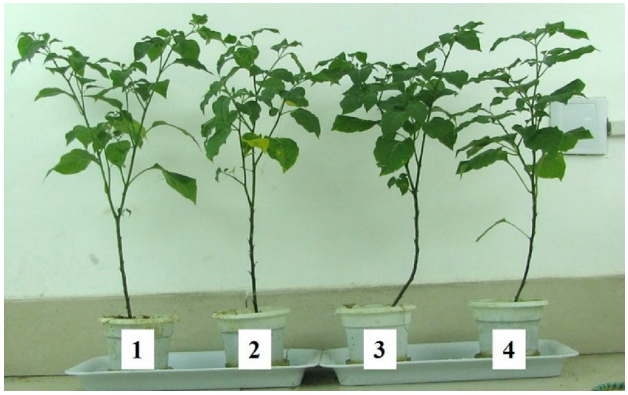

Fig. 10 Growth of *Solanum nigrum* L. within 8 weeks. Number 1 and 2 without Jute/SA residue but watered using Hoagland's nutrient solution. Number 3 and 4 with Jute/SA residue but watered using tap water

The disposal of spent adsorbents is an environmental concern. Considering the biodegradation of all-biomass Jute/SA, the spent Jute/SA adsorbent (after 10 cycles) was thoroughly washed with 0.1 mol L^{-1} HCl solution and water to remove residual heavy metals and used as fertilizer for plant growth in roseite cultivation medium. As shown in Fig. 10, the plant of *Solanum nigrum* L. grew well after being watered with tap water within 8 weeks (No. 3 and 4), which could rival those growing in roseite cultivation medium without Jute/SA residue but watered using Hoagland's nutrient solution (No. 1 and 2). After harvesting these plant, there were no heavy metals detected in the soil and the plant. So, the spent adsorbent could be used as a fertilizer in infertile soil for the cultivation of plant.

Treatment of Actual Melting Effluent

In order to evaluate the applicability of Jute/SA gel adsorbent, the metal adsorption efficiency was tested in an actual melting effluent. The suspended solid in the effluent was removed by filtration before test. The main metals are Pb, Cd, Zn, Cu, Mn, Ni and Fe with initial concentration of 7.539, 4.743, 43.95, 16.500, 19.24, 4.900 and 33.75 mg L^{-1}, respectively. Before adsorption, the initial pH was adjusted from 2.4 to 5.0. The adsorption efficiencies within 45 min are listed in Table 6. When using 1 g L^{-1} Jute/SA gel, the adsorption efficiencies of Pb, Cd, Zn, Cu, Mn, Ni and Fe ions were 99.1, 89.9, 54.7, 42.1, 28.5, 2.0 and 99.4%, respectively. In this process, Fe showed a relatively high removal efficiency, probably due to high average valence electron energy and the $3d^6 4s^2$ subshell, which offer empty orbital and strongly coordinate with active site [38]. When increasing adsorbent dose to 2 g L^{-1}, the adsorption efficiencies of Pb^{2+} and Cd^{2+} increased to 99.9% and 99.5%, respectively. When further increasing adsorbent dose to 4 g L^{-1}, the removal efficiencies of Pb^{2+} and Cd^{2+} reached almost 100% (the residual concentration was below 0.001 mg L^{-1}). Jute/SA gel shows a great potential in the treatment of industrial effluent containing heavy metals.

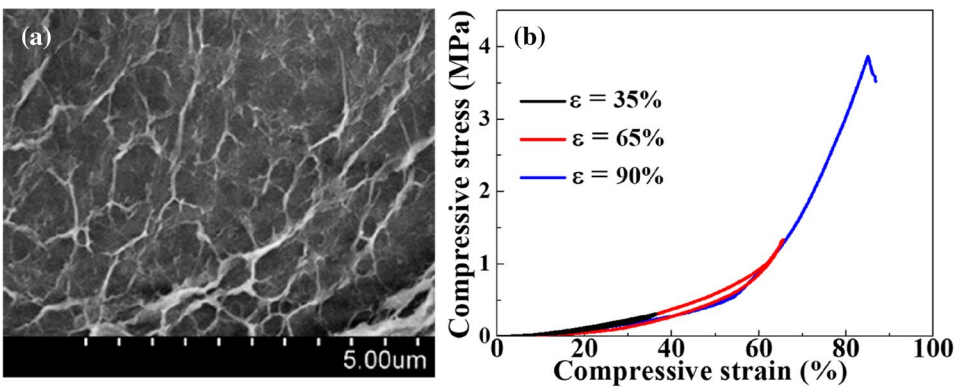

Fig. 9 SEM image (**a**) and the strain–stress curves (**b**) of freeze-dried Jute/SA gel after 10-cycling adsorption-desorption processes

Table 6 Treatment of melting effluent using Jute/SA gel

Adsorbent dose (g L^{-1})	pH	Metal ion concentration (mg L^{-1})						
		Pb^{2+}	Cd^{2+}	Zn^{2+}	Cu^{2+}	Mn^{2+}	Ni^{2+}	Fe^{2+}
0	2.4	7.539	4.743	43.95	16.500	19.24	4.900	33.75
1	5.0	0.067	0.48	19.91	9.550	13.75	4.800	0.21
2	5.0	0.011	0.026	17.15	5.607	10.75	3.875	< 0.01
3	5.0	< 0.001	0.003	15.05	3.550	9.75	3.600	< 0.01
4	5.0	< 0.001	< 0.001	13.6	2.150	7.75	3.250	< 0.01

Conclusions

This work develops a highly practical all-biomass hydrogel adsorbent. The double network structure and high water content of Jute/SA gel is conducive to improving metal ions diffusion, exposure of adsorption sites, and reusability. Jute/SA gel can be efficiently conducted in pH range of 3–6 and the adsorption kinetic equilibrium is fast. The adsorbent shows comparable adsorption capacities of Pb^{2+} and Cd^{2+} with those for the best adsorbents reported so far. Jute/SA gel is effective in removing Pb^{2+} and Cd^{2+} in actual melting effluent containing various metals. Meanwhile, Jute/SA gel can be easily regenerated and highly reused with an excellent recyclability. In addition, the spent Jute/SA hydrogel adsorbent was a good organic fertilizer.

Acknowledgements This work was supported by the National Natural Science Foundation of China (51778218), the Science and Technology Innovation Plan of Hunan Province (2019JJ10001, 2020JJ7036, 2017SK2420 and 2019RS3015) and Hunan Provincial Key Laboratory for Cost-effective Utilization of Fossil Fuel Aimed at Reducing Carbon-dioxide Emissions (HND2018005).

References

1. Liu Y, Xiao T, Baveye P, Zhu J, Ning Z, Li H (2015) Potential health risk in areas with high naturally-occurring cadmium background in southwestern China. Ecotoxicol Environ Saf 112:122–131
2. Uddin M (2017) A review on the adsorption of heavy metals by clay minerals, with special focus on the past decade. Chem Eng J 308:438–462
3. Shao P, Liang D, Yang L, Shi H, Xiong Z, Ding L, Yin X, Zhang K, Luo X (2020) Evaluating the adsorptivity of organo-functionalized silica nanoparticles towards heavy metals: quantitative comparison and mechanistic insight. J Hazard Mater 387:121676
4. Chitpong N, Husson S (2017) High-capacity, nanofiber-based ion-exchange membranes for the selective recovery of heavy metals from impaired waters. Sep Purif Technol 179:94–103
5. Ihsanullah A, Al-Amer A, Laoui T, Al-Marri M, Nasser M, Khraisheh M, Atieh M (2016) Heavy metal removal from aqueous solution by advanced carbon nanotubes: critical review of adsorption applications. Sep Purif Technol 157:141–161
6. Kyzas G, Bomis G, Kosheleva R, Efthimiadou E, Favvas E, Kostoglou M, Mitropoulos A (2019) Nanobubbles effect on heavy metal ions adsorption by activated carbon. Chem Eng J 356:91–97
7. Liu D, Li Z, Li W, Zhong Z, Xu J, Ren J, Ma Z (2013) Adsorption behavior of heavy metal ions from aqueous solution by soy protein hollow microspheres. Ind Eng Chem Res 52:11036–11044
8. Loganathan P, Shim W, Sounthararajah D, Kalaruban M, Nur T, Vigneswaran S (2018) Modelling equilibrium adsorption of single, binary, and ternary combinations of Cu, Pb, and Zn onto granular activated carbon. Environ Sci Pollut Res 25:16664–16675
9. Bumanis G, Novais R, Carvalheiras J, Bajare D, Labrincha J (2019) Metals removal from aqueous solutions by tailored porous waste-based granulated alkali-activated materials. Appl Clay Sci 179:105147
10. Shao P, Ding L, Luo J, Luo Y, You D, Zhang Q, Luo X (2019) Lattice-defect-enhanced adsorption of arsenic on zirconia nanospheres: A combined experimental and theoretical study. ACS Appl Mater Interfaces 11:29736–29745
11. Zhao G, Huang X, Tang Z, Huang Q, Niu F, Wang X (2018) Polymer-based nanocomposites for heavy metal ions removal from aqueous solution: a review. Polym Chem 9:3562–3582
12. Anastopoulos I, Robalds A, Nguyen Tran H, Mitrogiannis D, Giannakoudaki D, Hosseini-Bandegharaei A, Dotto G (2019) Removal of heavy metals by leaves-derived biosorbents. Environ Chem Lett 17:755–766
13. Lai Y, Chang Y, Chen M, Lo Y, Lai J, Lee D (2016) Poly(vinyl alcohol and alginate cross-linked matrix with immobilized Prussian blue and ion exchange resin for cesium removal from waters. Bioresour Technol 214:192–198
14. Zhou G, Luo J, Liu C, Chu L, Crittenden J (2018) Efficient heavy metal removal from industrial melting effluent using fixed-bed process based on porous hydrogel adsorbents. Water Res 131:246–254
15. Zhou G, Luo J, Liu C, Chu L, Ma J, Tang Y, Zeng Z, Luo S (2016) A highly efficient polyampholyte hydrogel sorbent based fixed-bed process for heavy metal removal in actual industrial effluent. Water Res 89:151–160
16. Rajamani M, Rajendrakumar K (2019) Chitosan-boehmite desiccant composite as a promising adsorbent towards heavy metal removal. J Environ Manag 244:257–264
17. Avetta P, Pensato A, Minella M, Malandrino M, Maurino V, Minero C, Hanna K, Vione D (2015) Activation of persulfate by irradiated magnetite: implications for the degradation of phenol under heterogeneous photo-fenton-like conditions. Environ Sci Technol 49:1043–1050
18. Mu B, Zhong W, Dong Y, Du P, Liu P (2012) Encapsulation of drug microparticles with self-assembled Fe_3O_4/alginate hybrid multilayers for targeted controlled release. J Biomed Mater Res B 100:825–831
19. Zhou G, Liu C, Chu L, Tang Y, Luo S (2016) Rapid and efficient treatment of wastewater with high-concentration heavy metals using a new type of hydrogel-based adsorption process. Bioresour Technol 219:451–457
20. Yang P, Zhao J, Zhang L, Li L, Zhu Z (2015) Intramolecular hydrogen bonds quench photoluminescence and enhance photocatalytic activity of carbon nanodots. Chem Eur J 21:8561–8568

21. Chu L, Liu C, Zhou G, Xu R, Tang Y, Zeng Z, Luo S (2015) A double network gel as low cost and easy recycle adsorbent: highly efficient removal of Cd(II) and Pb(II) pollutants from wastewater. J Hazard Mater 300:153–160
22. Hadi P, Barford J, McKay G (2013) Toxic heavy metal capture using a novel electronic waste-based material—mechanism, modeling and comparison. Environ Sci Technol 47:8248–8255
23. Petrus R, Warcho J (2005) Heavy metal removal by clinoptilolite. An equilibrium study in multi-component systems. Water Res 39:819–830
24. Phetphaisit C, Yuanyang S, Chaiyasith W (2016) Polyacrylamido-2-methyl-1-propane sulfonic acid-grafted-natural rubber as bioadsorbent for heavy metal removal from aqueous standard solution and industrial wastewater. J Hazard Mater 301:163–171
25. Xu R, Zhou G, Tang Y, Chu L, Liu C, Zeng Z, Luo S (2015) New double network hydrogel adsorbent: highly efficient removal of Cd(II) and Mn(II) ions in aqueous solution. Chem Eng J 275:179–188
26. Zhu Y, Hu J, Wang J (2012) Competitive adsorption of Pb(II), Cu(II) and Zn(II) onto xanthate-modified magnetic chitosan. J Hazard Mater 221:155–161
27. Sounthararajah D, Loganathan P, Kandasamy J, Vigneswaran S (2015) Adsorptive removal of heavy metals from water using sodium titanate nanofibers loaded onto GAC in fixed-bed columns. J Hazard Mater 287:306–316
28. El-Toni A, Habila M, Ibrahim M, Labis J, ALOthman Z (2014) Simple and facile synthesis of amino functionalized hollow core-mesoporous shell silica spheres using anionic surfactant for Pb(II), Cd(II), and Zn(II) adsorption and recovery. Chem Eng J 251:441–451
29. Deng S, Wang P, Zhang G, Dou Y (2016) Polyacrylonitrile-based fiber modified with thiosemicarbazide by microwave irradiation and its adsorption behavior for Cd(II) and Pb(II). J Hazard Mater 307:64–72
30. Liang X, Xu Y, Sun G, Wang L, Sun Y, Sun Y, Qin X (2011) Preparation and characterization of mercapto functionalized sepiolite and their application for sorption of lead and cadmium. Chem Eng J 174:436–444
31. Liu D, Li Z, Zhu Y, Li Z, Kumar R (2014) Recycled chitosan nanofibril as an effective Cu(II), Pb(II) and Cd(II) ionic chelating agent: adsorption and desorption performance. Carbohydr Polym 111:469–476
32. Ding Y, Liu Y, Liu S, Li Z, Tan X, Huang X, Zeng G, Zhou Y, Zheng B, Cai X (2016) Competitive removal of Cd(II) and Pb(II) by biochars produced from water hyacinths: performance and mechanism. RSC Adv 6:5223–5232
33. Cataldo S, Gianguzza A, Merli M, Muratore N, Piazzese D, Liveri M (2014) Experimental and robust modeling approach for Pb(II) uptake by alginate gel beads: Influence of the ionic strength and medium composition. J Colloid Interface Sci 434:77–88
34. He J, Lu Y, Luo G (2014) Ca(II) imprinted chitosan microspheres: an effective and green adsorbent for the removal of Cu(II), Cd(II) and Pb(II) from aqueous solutions. Chem Eng J 244:202–208
35. Sangi M, Shahmoradi A, Zolgharnein J, Azimi G, Ghorbandboost M (2008) Removal and recovery of heavy metals from aqueous solution using *Ulmus carpinifolia* and *Fraxinus excelsior* tree leaves. J Hazard Mater 155:513–522
36. Zhou G, Liu C, Tang Y, Luo S, Zeng Z, Liu Y, Xu R, Chu L (2015) Sponge-like polysiloxane-graphene oxide gel as a highly efficient and renewable adsorbent for lead and cadmium metals removal from wastewater. Chem Eng J 280:275–282
37. Wu N, Li Z (2013) Synthesis and characterization of poly(HEA/MALA) hydrogel and its application in removal of heavy metal ions from water. Chem Eng J 215–216:894–902
38. Srivastava S, Agrawal S, Mondal M (2015) A review on progress of heavy metal removal using adsorbents of microbial and plant origin. Environ Sci Pollut Res 22:15386–15415